4352–4359 *Nucleic Acids Research, 2011, Vol. 39, No. 10* *Published online 25 January 2011*
doi:10.1093/nar/gkq1359

Controlled interplay between trigger loop and Gre factor in the RNA polymerase active centre

Mohammad Roghanian, Yulia Yuzenkova and Nikolay Zenkin*

Centre for Bacterial Cell Biology, Institute for Cell and Molecular Biosciences, Newcastle University, Baddiley-Clark Building, Richardson Road, Newcastle upon Tyne, NE2 4AX, UK

Received November 16, 2010; Revised December 27, 2010; Accepted December 28, 2010

ABSTRACT

The highly processive transcription by multi-subunit RNA polymerases (RNAP) can be interrupted by misincorporation or backtracking events that may stall transcription or lead to erroneous transcripts. Backtracked/misincorporated complexes can be resolved via hydrolysis of the transcript. Here, we show that, in response to misincorporation and/or backtracking, the catalytic domain of RNAP active centre, the trigger loop (TL), is substituted by transcription factor Gre. This substitution turns off the intrinsic TL-dependent hydrolytic activity of RNAP active centre, and exchanges it to a far more efficient Gre-dependent mechanism of RNA hydrolysis. Replacement of the TL by Gre factor occurs only in backtracked/misincorporated complexes, and not in correctly elongating complexes. This controlled switching of RNAP activities allows the processivity of elongation to be unaffected by the hydrolytic activity of Gre, while ensuring efficient proofreading of transcription and resolution of backtracked complexes.

INTRODUCTION

The reactions performed by RNA polymerase (RNAP) were proposed to be catalysed by two distinct entities of the active centre: the two Mg^{2+} ions and a flexible domain of the active site, the trigger loop (TL). The two Mg^{2+} ions of the active centre [one of which (Mg^{2+}I) is chelated by the invariant aspartate triad, and another (Mg^{2+}II) is chelated by a substrate] are thought to catalyse phosphotransfer reactions via a general two Me^{2+} ion mechanism (1–3). The TL is involved in donating amino acids that directly participate in catalysis (4–9). Amino acids β′R1239 and β′H1242 (*Thermus aquaticus* numbering) of the TL of bacterial RNAP were proposed to stabilize the transition state of phosphodiester bond formation (and, presumably, of pyrophosphorolysis) (4,8). During phosphodiester bond hydrolysis by bacterial RNAP, β′H1242 of the TL participates in the reaction as a general base, though β′H1242 may also be required to orient the 3′-end NMP of the transcript that assists hydrolysis (9). The magnitude of effects of the deletion of the TL on catalysis by bacterial RNAP (4,8–10) is close to that of substitutions in the aspartate triad which chelates Mg^{2+}I (11), pointing out the central role of the TL, along with the Mg^{2+} ions, in RNAP activity. The TL of eukaryotic RNAP II is also essential for phosphodiester bond synthesis, though the mechanism by which the TL participates in catalysis may be different from that of bacterial RNAPs (6,12). The role of the TL of RNAP II in hydrolysis has not been investigated.

Taken together, the existing data indicate that the Mg^{2+} ions and the TL together form the active centre of RNAP. However, while the configuration of the aspartate triad remains constant, the TL may exist in a catalytically competent, folded state and in an inactive, unfolded state (4,5,7). In the unfolded state, the catalytic residues β′R1239 and β′H1242 are too far from the reactants to participate in catalysis (Figure 1A). Folding of the TL brings them to a catalytically active position (Figure 1A). Such an ability to bring and remove one of the two parts of the active centre may serve as a mechanism to provide fidelity for RNA synthesis (4), adaptation and possibly regulation of RNAP catalytic activities (13).

Hydrolysis of RNA by bacterial RNAP is known to be stimulated by the transcription factor Gre (note that *T. aquaticus* used below has only one Gre factor; in contrast, *Escherichia coli* has two Gre factors: GreA and GreB) (14–19). Two acidic residues, D42 and E45 (*T. aquaticus* numbering), of the Gre coiled-coil domain which was proposed to protrude through RNAP's secondary channel, are thought to fix the second catalytic Mg^{2+} ion in the active centre (17,18,20). Given that the TL and Gre factor both assist RNA hydrolysis, they have to either

*To whom correspondence should be addressed. Tel: +44(0)1912083227; Fax: +44(0)1912083205; Email: n.zenkin@ncl.ac.uk

The authors wish it to be known that, in their opinion, the first two authors should be regarded as joint First Authors.

cooperate or compete with each other in the process. Recently, it was proposed that the TL of *E. coli* RNAP was not required for Gre assisted hydrolysis (8). However, in the same study, the TL was also dispensable for factor-independent intrinsic hydrolysis (8). In a more recent work, the TL was shown to be essential for phosphodiester bond hydrolysis by *T. aquaticus* and *E. coli* RNAPs on both, assembled backtracked complexes and complexes that undergone 'natural' backtracking through misincorporation (9), suggesting that the experimental system used by Zhang *et al.* (8) was unsuitable for investigating RNAP hydrolytic reactions. In a different study, mutants of *E. coli* GreB, deficient in cleavage, were shown to inhibit some intrinsic activities of RNAP (17), suggesting that GreB may somehow interfere with the arrangement of the active centre. Thus, the mechanisms of collaboration between the TL and Gre in the secondary channel remain unclear. Furthermore, Gre factor is thought to always accompany RNAP as a transient catalytic component (17). This raises a question of how the polymerase activity of the RNAP active centre and the Gre assisted RNA hydrolysis co-exist, and how their exchange is regulated during transcription elongation to allow efficient and highly accurate RNA synthesis.

Here, we show that Gre factor can substitute for the TL in the active centre thus switching off the TL catalysed hydrolytic activity and instead remodelling the active centre into a highly efficient nuclease. Such replacement of active centres takes place only in response to backtracking or misincorporation events, thus explaining how activity of Gre factor is regulated.

MATERIALS AND METHODS

Mutant RNAP construction and purification

Thermus aquaticus RNAPs lacking the TL (β′ residues 1238–1245) or bearing alanine substitution of H1242 of the TL were constructed as described (4,10). WT and mutant core RNA polymerases were purified as described (9,21). The plasmid expressing *T. aquaticus* Gre factor (pET28A derivative) was a gift from L. Minakhin. Mutant Gre factor bearing alanine substitutions of D42 and E45, $Gre^{D42A/E45A}$, was obtained by site-directed mutagenesis. WT and the mutant Gre factors were purified as described (19).

Transcription assays

Elongation complexes were assembled with RNA radioactively labelled at the 5′-end as described (14), except for complexes were immobilized on streptavidin agarose beads (Fluka) through biotin of the 5′-end of DNA template strand. Sequences of oligonucleotides used for the elongation complexes assembly are shown in Figure 1B. cEC15 was obtained from cEC13 by walking RNAP by two positions by the addition of 10 μM ATP, 10 μM GTP and 10 mM $MgCl_2$ (final concentration) and their subsequent removal by washing of immobilized complexes with transcription buffer. Transcription buffer contained 40 mM KCl and 20 mM Tris–HCl pH 7.9, unless otherwise specified. Reactions were started by the addition of 10 mM $MgCl_2$ (final concentration) with or without NTP (final concentration specified in figures and figure legends) or 0.5 mM pyrophosphate. Gre or $Gre^{D42A/E45A}$ were added prior to the start of the reaction for 1 min. All reactions were performed at 40°C, apart from Gre catalysed cleavage which was performed at 20°C to reduce rate of cleavage for manual measurements. The reactions were stopped by addition of loading buffer containing formamide. Products were resolved in denaturing 23% PAGE (8 M Urea), revealed by PhosphorImaging (GE Healthcare) and analysed using ImageQuant software (GE Healthcare). Kinetic data were fitted to a single or double exponential equation using non-linear regression in SigmaPlot (9,14). To determine $K_m[Mg^{2+}]$ for cleavage in mEC15 the reaction rates obtained in various $MgCl_2$ concentrations were fitted to the Michaelis–Menten equation (9,14).

Exonuclease III footprinting

Exonuclease III (Exo III) footprinting of the front edge of RNAP was performed as described (10). cEC13 and cEC15 were obtained as above with the only exception that the downstream DNA was 14 bp longer and the non-template strand was ^{32}P labelled at the 5′-end. RNA was also ^{32}P labelled at the 5′-end. ExoIII (1, 10 or 100 U) (New England Biolabs) were added to reactions together with 5 mM $MgCl_2$ final concentration, followed by 1 min incubation at 40°C before addition of stop solution. Products were analysed as above.

RESULTS

The TL and Gre catalyse phosphodiester bond hydrolysis via distinct mechanisms

To investigate how the TL and Gre cooperate to catalyse phosphodiester bond hydrolysis we used wild-type *T. aquaticus* RNAP (WT RNAP) and a mutant RNAP lacking the TL (ΔTL RNAP) (4,9,10). Intrinsic phosphodiester bond hydrolysis by the active centre of RNAP proceeds at the second phosphodiester bond from the 3′-end of the transcript, and is assisted by the NMP at the 3′-end of the RNA (14). However, the rate of the reaction also depends on the translocation state of the elongation complex (14). Therefore, we analysed cleavage reactions in the misincorporated elongation complex 'mEC15′ of which the 3′ NMP of the RNA was non-complementary to the corresponding template base (Figure 1B) (9,14). These complexes are stabilized in 1 bp backtracked conformation, thus eliminating possible translocation effects on the rate of phosphodiester bond hydrolysis. These constructs have been shown to be indistinguishable in hydrolytic reactions from complexes brought to 1 base pair backtracked state via 'natural' misincorporation (9).

As expected, deletion of the TL had a drastic effect on intrinsic cleavage (Figure 1C), supporting our previous conclusions that the TL is essential for this reaction (9). The effect of the TL deletion on intrinsic cleavage was not due to the altered affinity of RNAP to Mg^{2+} (Figure 1E) which is chelated by the 3′-end NMP of the RNA

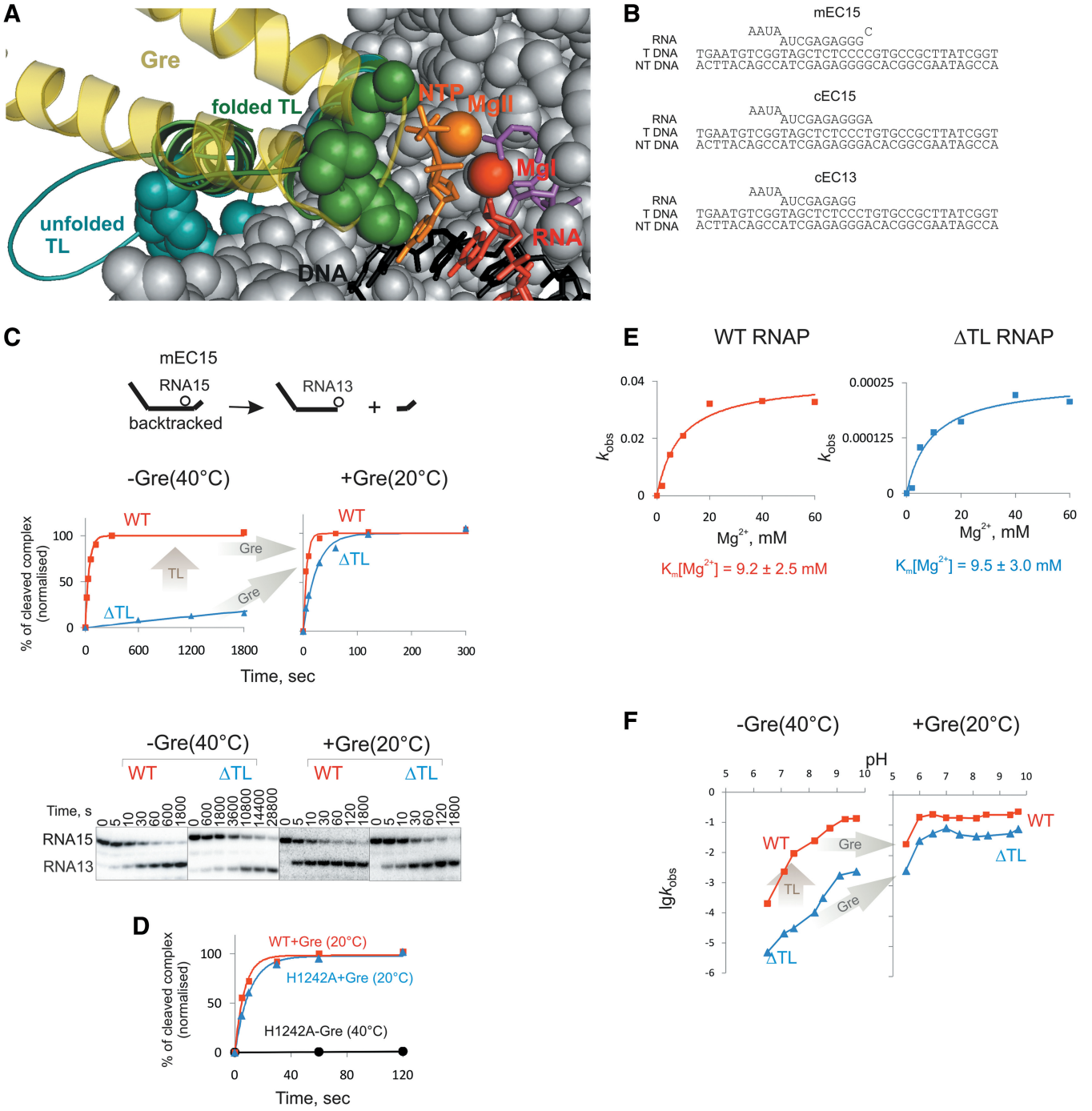

Figure 1. (**A**) Upon folding the TL forms part of the RNAP active centre. The TL of *T. thermophilus* RNAP [PDB 2BE5 and 2O5J, respectively (7,34)], which has complete conservation with the active centre amino acids of *T. aquaticus* RNAP used in our study, in unfolded and folded states is coloured green and cyan, respectively. The amino acids of the TL that form the 'TL active centre' upon TL folding (M1238, R1239, H1242, T1243) are shown in space fill in both folded and unfolded states of the TL. The amino acids (not belonging to the TL) that surround catalytic Mg^{2+} ions and the incoming NTP are shown in grey spacefill. The aspartate triad is shown as purple sticks. Mg^{2+} ions of the active centre are shown as spheres. Incoming NTP, RNA 3′-end and DNA template bases are shown as orange, red and black sticks, respectively. The N-terminal coiled-coil domain of Gre factor (structure of *E. coli* GreA was used; PDB 1GRJ) which, according to our results, substitutes for the TL upon misincorporation or backtracking (see main text), was positioned to reach the active centre of RNAP without significant clashes with surrounding structure, and is shown as yellow ribbons. (**B**) Elongation complexes used in this study. Shown are the sequences of RNA, template strand (T DNA) and non-template strand (NT DNA) used to assemble elongation complexes (see 'Materials and Methods' section). (**C**) Gre-catalysed hydrolysis is independent of the TL. Kinetics of the cleavage reaction (also schematically shown above the plots) in mEC15 (Figure 1B) by WT RNAP (red) and ΔTL RNAP (blue), in the absence (left) or presence (right) of Gre factor. Solid curves are the single exponential fits of the kinetics data (see 'Materials and Methods' section). The grey arrows represent the contributions of the TL and Gre to the rate of the reaction. Representative gels for cleavage by WT and ΔTL RNAPs in the absence or the presence of Gre are shown below the plots. Note that the kinetics of Gre catalysed reactions were measured at 20°C to reduce the rate of the reaction to allow it to be measured manually. (**D**) Gre-catalysed hydrolysis is independent of the H1242 of the TL. Kinetics of the cleavage reaction in mEC15 (as in panel C) by H1242A RNAP with and without Gre, and WT RNAP with Gre. Solid curves are the single

(continued)

(9,14). Unexpectedly, in the presence of Gre, the cleavage was only slightly affected by the deletion of the TL (Figure 1C). Furthermore, alanine substitution of β′ H1242 of the TL (H1242A RNAP), which solely determines TL function in hydrolysis (9), had almost no effect on Gre assisted cleavage (Figure 1D). These results indicate that Gre assisted cleavage does not require presence of the TL, and suggest that Gre assisted cleavage proceeds via a mechanism different to that of TL-catalysed cleavage. The slightly slower rate of Gre assisted cleavage by ΔTL RNAP can be explained by minor structure disturbance caused by the deletion of the whole TL.

To test if the TL and Gre participate in phosphodiester bond hydrolysis via different mechanisms we examined the pH dependence of non-assisted (by ΔTL RNAP), TL-catalysed (WT RNAP) and Gre-catalysed (WT RNAP + Gre; ΔTL RNAP + Gre) cleavage reactions (Figure 1F). As expected, the TL increased the rate of non-assisted hydrolysis at all pH tested, and slightly changed the pH profile of the reaction (Figure 1F) (9). However, the pH profiles of Gre-catalysed cleavage by both WT and ΔTL RNAPs were similar to each other, and different from either non-assisted or TL-catalysed cleavage reactions (Figure 1F). The difference between the pH profiles of intrinsic and Gre assisted cleavage by WT RNAP is consistent with previous observations, and can be attributed to stabilization of the attacking hydroxyl by amino acids of the Gre N-terminal domain (19). We therefore conclude that Gre imposes its own mechanism of cleavage to the active centre which is independent of the TL, and that the TL does not participate in the Gre-catalysed hydrolysis.

Gre substitutes for the TL in the active centre

The above results suggest that, while acting in the active centre, Gre should switch off the TL catalysed cleavage. This may happen through physical blocking of TL folding upon Gre binding in the secondary channel. To test this hypothesis we used a mutant Gre factor that had two of the residues essential for catalysis [D42 and E45 (17,18)] changed to alanines, $Gre^{D42A/E45A}$. As seen from Figure 2A, addition of $Gre^{D42A/E45A}$ strongly inhibited the intrinsic cleavage (~30-fold). Cleavage by ΔTL RNAP was not affected by $Gre^{D42A/E45A}$ (Figure 2A). We cannot exclude the possibility that the deletion of the TL affects binding of $Gre^{D42A/E45A}$ to ΔTL RNAP. However, only slightly unaltered activity of the wild-type Gre with ΔTL RNAP argues that binding of the mutant Gre to ΔTL RNAP in a functional conformation is not affected significantly (see previous section). The results, therefore, indicate that, upon binding, Gre factor indeed inactivates the TL and thus turns off the intrinsic cleavage activity of the RNAP. The lack of full inactivation of TL dependent hydrolysis by $Gre^{D42A/E45A}$ (to the level of hydrolysis rate by ΔTL RNAP) can be explained by temporary dissociation of $Gre^{D42A/E45A}$ from the elongation complex during long incubations, which presumably allows the TL to assist hydrolysis. Since the folded TL, along with Mg^{2+} ions, forms the active centre of RNAP, Gre substitution of the TL leads to *exchange* of the amino acid content and, as a result, of the catalytic properties of RNAP active centre. Therefore, this can be considered a substitution of the active centres of RNAP (see schemes in Figures 1A and 3).

Gre action in the active centre is controlled by the conformation of the elongation complex

As we have shown previously, all activities of RNAP depend on the TL (4,9). Since Gre binding switches off one of them (intrinsic hydrolytic activity), Gre might also switch off other TL dependent activities. If so, addition of $Gre^{D42A/E45A}$ to reactions catalysed by WT RNAP should inhibit them. To test this, we analysed single NTP addition in a correct elongation complex (cEC15, which was identical to mEC15 but had the 3′-end of the transcript correctly paired with template DNA; Figure 1B). Interestingly, $Gre^{D42A/E45A}$ inhibited NTP addition only in a fraction of complexes, while the rest of the complexes were unaffected (Figure 2B). Partial inhibition of the complexes was not due to the altered affinity to NTP since the same fractionation of complexes was observed with a higher NTP concentration (Figure 2B, right panel).

As a result of thermal oscillation of elongation complex between translocation states cEC15 may occasionally backtrack. We hypothesized that Gre brings its activity only in elongation incompetent, backtracked, complexes and in the active complexes it does not interfere with the active centre. This would explain why NTP addition is inhibited by $Gre^{D42A/E45A}$ only in a fraction of cEC15. To test this hypothesis, we analysed the effects of $Gre^{D42A/E45A}$ on the addition of NTP in an elongation complex stabilized in the transcriptionally active post-translocated conformation (cEC13 in Figure 1B). The relative translocational distribution in cEC13 and cEC15 was confirmed by measuring the rates of pyrophosphorolysis and second phosphodiester bond hydrolysis in these complexes and by Exo III footprinting (Figure 2C and D). Rates of pyrophosphorolysis and second phosphodiester bond hydrolysis directly depend on the shift of the translocation equilibrium of the elongation complex to pre-translocated and 1 bp backtracked states, respectively. cEC13 was very slow in both reactions indicating that it is stabilized in the post-translocated state (Figure 2C). In contrast, cEC15 underwent relatively fast pyrophosphorolysis and second phosphodiester bond

Figure 1. Continued
exponential fits of the kinetics data (see 'Materials and Methods' section). (**E**) The TL is not involved in Mg^{2+} chelation during phosphodiester bond hydrolysis. Dependence of k_{obs} on the Mg^{2+} concentration during intrinsic cleavage (as in panel C) by WT (red) and ΔTL (blue) RNAPs. The values of apparent $K_m[Mg^{2+}]$ are shown below the plots. The values of k_{obs} at different Mg^{2+} concentrations were calculated by single exponential fitting of the kinetics data (as in panel C) and $K_m[Mg^{2+}]$ values were calculated as described in 'Materials and Methods' section. (**F**) pH profiles of the reactions described in panel C in the absence and the presence of Gre. The values of k_{obs} at different pH were calculated by single exponential fitting of the kinetics data (see panel C and 'Materials and Methods' section). Note that reactions with Gre were performed at 20°C (as in panel C).

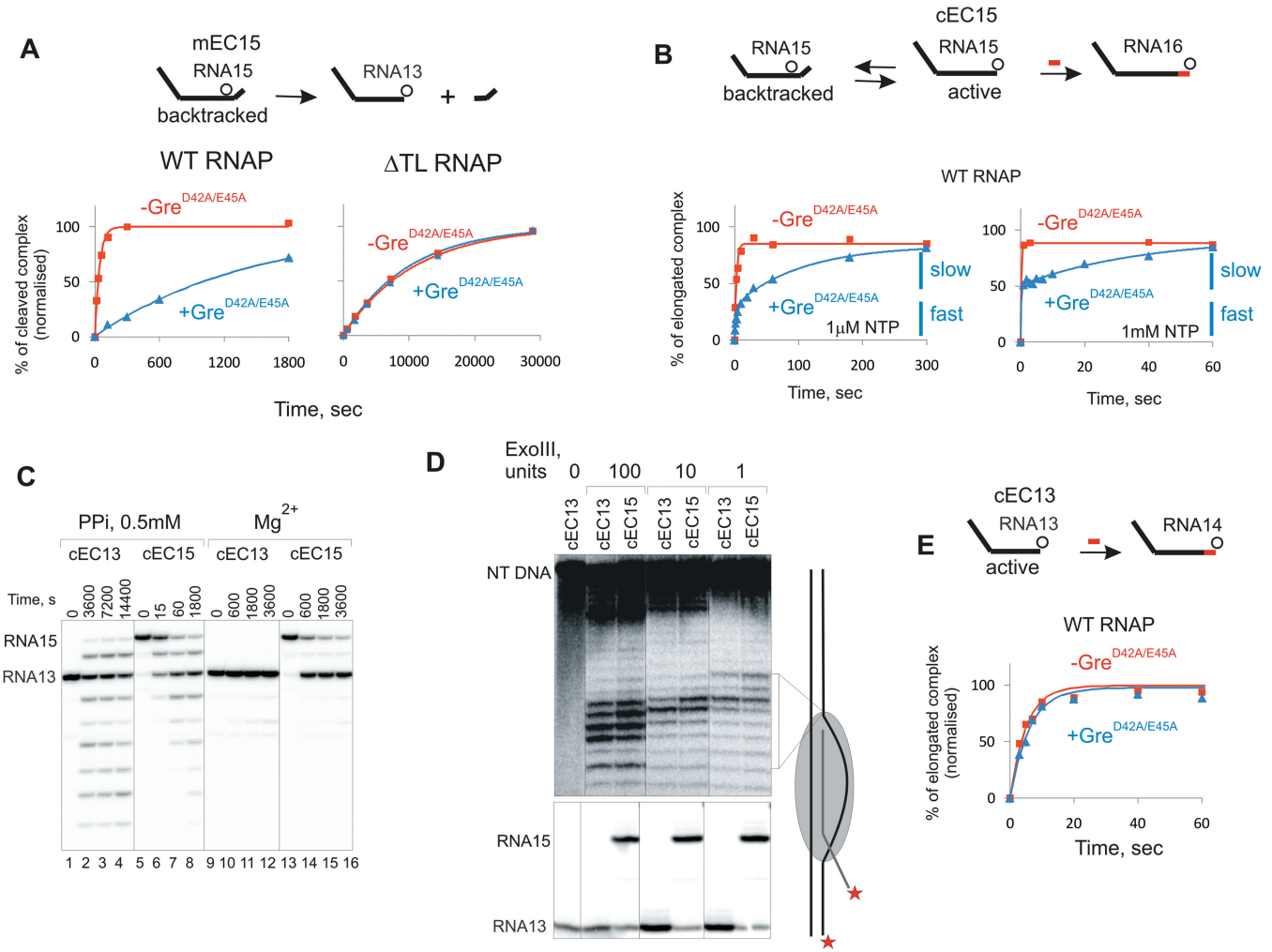

Figure 2. Substitution of the TL by Gre depends on the state of the elongation complex. (**A**) Kinetics of the cleavage reaction (schematically shown above the plots) in mEC15 (Figure 1B) by WT RNAP (left) and ΔTL RNAP (right) in the absence (red) or presence (blue) of the catalytically inactive mutant Gre factor, $Gre^{D42A/E45A}$. Solid curves are the single exponential fits of the kinetics data (see 'Materials and Methods' section). (**B**) Kinetics of single nucleotide addition (1 μM and 1 mM CTP; reaction schematically shown above the plots) in cEC15 (Figure 1B) by WT RNAP in the absence (red) or presence (blue) of $Gre^{D42A/E45A}$. Solid curves are the single (without $Gre^{D42A/E45A}$) or double (with $Gre^{D42A/E45A}$) exponential fits of the kinetics data (see 'Materials and Methods' section). Blue vertical lines in the left plot show the inhibited (slow) and non-inhibited (fast) fractions of elongation complexes. (**C**) Kinetics of pyrophosphorolysis and second phosphodiester bond hydrolysis in cEC13 and cEC15. RNAs longer than 13 nt in lanes 2–4 originate from incorporation of NTPs, which are the result of pyrophosphorolysis. (**D**) Exo III footprinting of the front edge of RNAP in cEC13 and cEC15. Non-template DNA strand (NT DNA) and RNA were labelled with P^{32} at the 5′-end (asterisks in the scheme on the left). Three different concentrations of Exo III were used for accurate comparison of relative distribution of translocation states in cEC13 and cEC15. The lower panel originates from the same gel as the top panel, and shows the transcripts in the complexes. Black vertical lines in both panels separate lanes originating from the same gel that were brought together. (**E**) Kinetics of single nucleotide addition (1 μM GTP, reaction schematically shown above the plots) in cEC13 (Figure 1B) by WT RNAP in the absence (red) or presence (blue) of the $Gre^{D42A/E45A}$. Solid curves are the single exponential fits of the kinetics data (see 'Materials and Methods' section).

hydrolysis (Figure 2C), indicating that oscillation of this complex frequently brings it to pre-translocated and to one base pair backtracked states. Note, however, that hydrolysis in cEC15 proceeded slower than in mEC15 indicating that cEC15 is not stabilized in the 1 bp backtracked state-like mEC15. For footprinting of the front edge of RNAP in cEC13 and cEC15, we used three different concentrations of Exo III. This is analogous to the analysis of the kinetics of Exo III digestion, which is essential for comparison of distribution between translocation states in different complexes (22,23). If cEC13 and cEC15 were in similar translocation states, one would expect a 2 bp shift of the Exo III footprint in these complexes. However, as seen from Figure 2D, the front edge of RNAP in cEC15 is shifted backwards, which is consistent with the idea that cEC15 oscillates between post-translocated and backtracked states. Together with the data on the rates of the reactions in cEC13 and cEC15, this result suggests that cEC15 does occasionally backtrack, while cEC13 is stabilized in the post-translocation state.

In agreement with the hypothesis that Gre inhibits TL dependent functions only in backtracked complexes, $Gre^{D42A/E45A}$ did not inhibit NTP addition in cEC13

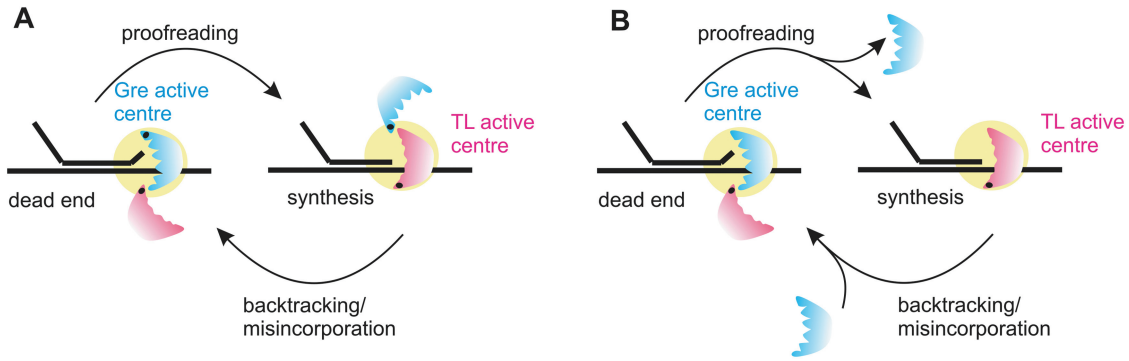

Figure 3. Two models of switching of the active centres, the 'TL active centre' (red) and 'Gre active centre' (blue), in the RNA polymerase catalytic site (yellow circle). Gre does not interfere with the TL during productive elongation. However, in response to misincorporation or occasional backtracking Gre substitutes for the TL in the active site where it activates the hydrolytic activity to efficiently resolve backtracked complexes. After resolution of backtracked complex is accomplished, Gre is replaced back by the TL allowing continuation of elongation. Switching may take place without (**A**) or with (**B**) dissociation of Gre from the elongation complex.

even at a low (1 μM) NTP concentration (Figure 2E). Therefore, only in response to misincorporation and/or backtracking events does Gre substitute for the TL in the active centre, thus modifying RNAP hydrolytic activity to efficiently resolve such dead end complexes. Active elongation complexes, however, lack the signal for substitution of the 'TL active centre' with the 'Gre active centre'. Therefore, in active elongation complexes Gre neither turns off TL-dependent catalysis, nor imposes cleavage activity, thus allowing continuous efficient transcript elongation. We cannot distinguish if the interplay between Gre and the TL takes place without dissociation of Gre from elongation complex or Gre has a higher affinity for backtracked than for correct complexes. Though it was proposed that Gre stays permanently bound to RNAP as its catalytic domain (17), these authors did not investigate binding to elongation complexes. We present two models, schematically shown in Figure 3, which are consistent with our results.

DISCUSSION

In this study, we show that during misincorporation and/or backtracking, the TL of the active centre is substituted by Gre factor, which 'turns off' TL-dependent hydrolytic activity and 'turns on' a much more efficient Gre-dependent hydrolytic activity. Substitution of the TL by Gre leads to reversible replacement of the amino acid content of the active centre, and this can be regarded as an 'exchange' of a part of the active centre. The exchange of RNAP 'polymerase' (TL) and 'nuclease' (Gre) active centres occurs in the single site of the enzyme without shifting of reactants in space, which is different from DNA polymerase (DNAP) proofreading activity. DNAP can switch between its 'polymerase' and 'proofreading' activities by moving the DNA product for a distance of up to 40 Å between two individual domains (24).

Second principal finding of our study is that the switch between the TL and Gre in the active centre takes place in a controlled manner in response to specific signals: backtracking and/or misincorporation and their resolution. The signal for replacement of the active centres in RNAP is presumably based on a conformational change of the protein that allows Gre to change its orientation and enter the secondary channel of RNAP. The main binding site of Gre is the β′ coiled coil situated at the entrance of the secondary channel, where C-terminal domain of Gre binds (25). A possible change in the orientation of this coiled coil, which may be dependent on the conformation of the TL, may drag Gre in and out of the secondary channel. This idea is supported by crystallographic studies that revealed small conformational changes in the vicinity of the active centre in various states of the elongation complex (7,26,27). Alternatively, the conformational change may occur in Gre. This idea may be supported by findings that a Gre homologue Gfh1 changes the orientation of its coiled-coil domain relative to the C-terminal domain, in a pH-dependent manner (28,29).

The controlled manner of switching of the TL and Gre active centres (only in response to misincorporation or backtracking) allows Gre-catalysed RNA cleavage to be as rapid as RNA synthesis catalysed by the TL. Indeed, the rate of Gre-catalysed hydrolysis (0.17 s^{-1} at 20°C) is close to the rate of phosphodiester bond formation in saturating NTP concentrations (0.61 s^{-1} at 20°C). As was proposed previously (17), Gre always accompanies RNAP in the cell (17). Therefore, if Gre activity is not controlled, and Gre is allowed to act in correct elongation complexes, inhibition of synthesis via inactivation of the TL and fast Gre-catalysed hydrolysis would lead to a rapid degradation of nascent transcripts, thus inhibiting transcription. This controlled manner of proofreading is different to the one used by DNAP, whose proofreading relies on the slowing down of chain extension upon misincorporation, which provides time for exonuclease domain to excise the erroneous nucleotide (24). Our results also reveal the principal difference between Gre-catalysed and transcript-assisted mechanisms of proofreading. The latter, as in the case of DNAP, also depends on the delay in the transcript extension after misincorporation event, allowing sufficient time for correcting a mistake (14).

Inhibition or activation of enzymatic activity by interfering with amino acid contents of their active centres by other proteins is a common way of regulation of proteinaceous enzymes (30,31). However, the controlled exchange of the activities via substitution of a part of an active centre may be a unique property of multi-subunit RNAPs. The abundance of factors (and potential factors) and small molecules that bind to RNAP in the secondary channel (GreA, GreB, Gfh1, DksA, Rnk, TraR, ppGpp, Tagetitoxin, Streptolydigin, Microcin J25—in bacteria; TFIIS, RNAP II subunit B12.2, RNAP I subunit A12.6, RNAP III subunit C11, α-amanitin—in eukaryotes) suggests that the on/off switching and exchanging of the activities via substitutions of a part of the active centre might be a common way of regulating RNAP activities. This idea is supported by the crystal structures of the elongation complexes with eukaryotic cleavage factor TFIIS (27,32) and RNAP inhibitor α-amanitin (5,26), in which the TL is in the unfolded conformation, and is being substituted by the factor or antibiotic, respectively. Recently, in analogy with the results of our study, it was shown that mutant TFIIS deficient in cleavage inhibits RNAP II activity (33). Our results suggest that this happens due to substitution of the TL by the mutant factor and, as a result, inhibition of the TL-catalysed reactions.

ACKNOWLEDGEMENTS

We thank Kathryn Doris and Richard Daniel for critical reading of the manuscript.

FUNDING

Funding for open access charge: UK Biotechnology and Biological Sciences Research Council; European Research Council (ERC-2007-StG 202994-MTP to N.Z.).

Conflict of interest statement. None declared.

REFERENCES

1. Zaychikov,E., Martin,E., Denissova,L., Kozlov,M., Markovtsov,V., Kashlev,M., Heumann,H., Nikiforov,V., Goldfarb,A. and Mustaev,A. (1996) Mapping of catalytic residues in the RNA polymerase active center. *Science*, **273**, 107–109.
2. Steitz,T.A. (1998) A mechanism for all polymerases. *Nature*, **391**, 231–232.
3. Sosunov,V., Sosunova,E., Mustaev,A., Bass,I., Nikiforov,V. and Goldfarb,A. (2003) Unified two-metal mechanism of RNA synthesis and degradation by RNA polymerase. *EMBO J.*, **22**, 2234–2244.
4. Yuzenkova,Y., Bochkareva,A., Tadigotla,V.R., Roghanian,M., Zorov,S., Severinov,K. and Zenkin,N. (2010) Stepwise mechanism for transcription fidelity. *BMC Biol.*, **8**, 54.
5. Kaplan,C.D., Larsson,K.M. and Kornberg,R.D. (2008) The RNA polymerase II trigger loop functions in substrate selection and is directly targeted by alpha-amanitin. *Mol. Cell*, **30**, 547–556.
6. Wang,D., Bushnell,D.A., Westover,K.D., Kaplan,C.D. and Kornberg,R.D. (2006) Structural basis of transcription: role of the trigger loop in substrate specificity and catalysis. *Cell*, **127**, 941–954.
7. Vassylyev,D.G., Vassylyeva,M.N., Zhang,J., Palangat,M., Artsimovitch,I. and Landick,R. (2007) Structural basis for substrate loading in bacterial RNA polymerase. *Nature*, **448**, 163–168.
8. Zhang,J., Palangat,M. and Landick,R. (2009) Role of the RNA polymerase trigger loop in catalysis and pausing. *Nat. Struct. Mol. Biol.*, **17**, 99–104.
9. Yuzenkova,Y. and Zenkin,N. (2010) Central role of the RNA polymerase trigger loop in intrinsic RNA hydrolysis. *Proc. Natl Acad. Sci. USA*, **107**, 10878–10883.
10. Temiakov,D., Zenkin,N., Vassylyeva,M.N., Perederina,A., Tahirov,T.H., Kashkina,E., Savkina,M., Zorov,S., Nikiforov,V., Igarashi,N. *et al.* (2005) Structural basis of transcription inhibition by antibiotic streptolydigin. *Mol. Cell*, **19**, 655–666.
11. Sosunov,V., Zorov,S., Sosunova,E., Nikolaev,A., Zakeyeva,I., Bass,I., Goldfarb,A., Nikiforov,V., Severinov,K. and Mustaev,A. (2005) The involvement of the aspartate triad of the active center in all catalytic activities of multisubunit RNA polymerase. *Nucleic Acids Res.*, **33**, 4202–4211.
12. Castro,C., Smidansky,E.D., Arnold,J.J., Maksimchuk,K.R., Moustafa,I., Uchida,A., Gotte,M., Konigsberg,W. and Cameron,C.E. (2009) Nucleic acid polymerases use a general acid for nucleotidyl transfer. *Nat. Struct. Mol. Biol.*, **16**, 212–218.
13. Miropolskaya,N., Artsimovitch,I., Klimasauskas,S., Nikiforov,V. and Kulbachinskiy,A. (2009) Allosteric control of catalysis by the F loop of RNA polymerase. *Proc. Natl Acad. Sci. USA*, **106**, 18942–18947.
14. Zenkin,N., Yuzenkova,Y. and Severinov,K. (2006) Transcript-assisted transcriptional proofreading. *Science*, **313**, 518–520.
15. Borukhov,S., Sagitov,V. and Goldfarb,A. (1993) Transcript cleavage factors from E. coli. *Cell*, **72**, 459–466.
16. Orlova,M., Newlands,J., Das,A., Goldfarb,A. and Borukhov,S. (1995) Intrinsic transcript cleavage activity of RNA polymerase. *Proc. Natl Acad. Sci. USA*, **92**, 4596–4600.
17. Laptenko,O., Lee,J., Lomakin,I. and Borukhov,S. (2003) Transcript cleavage factors GreA and GreB act as transient catalytic components of RNA polymerase. *EMBO J.*, **22**, 6322–6334.
18. Sosunova,E., Sosunov,V., Kozlov,M., Nikiforov,V., Goldfarb,A. and Mustaev,A. (2003) Donation of catalytic residues to RNA polymerase active center by transcription factor Gre. *Proc. Natl Acad. Sci. USA*, **100**, 15469–15474.
19. Laptenko,O. and Borukhov,S. (2003) Biochemical assays of Gre factors of Thermus thermophilus. *Methods Enzymol.*, **371**, 219–232.
20. Opalka,N., Chlenov,M., Chacon,P., Rice,W.J., Wriggers,W. and Darst,S.A. (2003) Structure and function of the transcription elongation factor GreB bound to bacterial RNA polymerase. *Cell*, **114**, 335–345.
21. Kuznedelov,K., Minakhin,L. and Severinov,K. (2003) Preparation and characterization of recombinant Thermus aquaticus RNA polymerase. *Methods Enzymol.*, **370**, 94–108.
22. Kireeva,M.L., Nedialkov,Y.A., Cremona,G.H., Purtov,Y.A., Lubkowska,L., Malagon,F., Burton,Z.F., Strathern,J.N. and Kashlev,M. (2008) Transient reversal of RNA polymerase II active site closing controls fidelity of transcription elongation. *Mol. Cell*, **30**, 557–566.
23. Kireeva,M.L. and Kashlev,M. (2009) Mechanism of sequence-specific pausing of bacterial RNA polymerase. *Proc. Natl Acad. Sci. USA*, **106**, 8900–8905.
24. Kunkel,T.A. and Bebenek,K. (2000) DNA replication fidelity. *Annu. Rev. Biochem.*, **69**, 497–529.
25. Vassylyeva,M.N., Svetlov,V., Dearborn,A.D., Klyuyev,S., Artsimovitch,I. and Vassylyev,D.G. (2007) The carboxy-terminal coiled-coil of the RNA polymerase beta'-subunit is the main binding site for Gre factors. *EMBO Rep.*, **8**, 1038–1043.
26. Brueckner,F. and Cramer,P. (2008) Structural basis of transcription inhibition by alpha-amanitin and implications for RNA polymerase II translocation. *Nat. Struct. Mol. Biol.*, **15**, 811–818.
27. Wang,D., Bushnell,D.A., Huang,X., Westover,K.D., Levitt,M. and Kornberg,R.D. (2009) Structural basis of transcription: backtracked RNA polymerase II at 3.4 angstrom resolution. *Science*, **324**, 1203–1206.

28. Symersky,J., Perederina,A., Vassylyeva,M.N., Svetlov,V., Artsimovitch,I. and Vassylyev,D.G. (2006) Regulation through the RNA polymerase secondary channel. Structural and functional variability of the coiled-coil transcription factors. *J. Biol. Chem.*, **281**, 1309–1312.
29. Laptenko,O., Kim,S.S., Lee,J., Starodubtseva,M., Cava,F., Berenguer,J., Kong,X.P. and Borukhov,S. (2006) pH-dependent conformational switch activates the inhibitor of transcription elongation. *EMBO J.*, **25**, 2131–2141.
30. Mattison,K., Wilbur,J.S., So,M. and Brennan,R.G. (2006) Structure of FitAB from Neisseria gonorrhoeae bound to DNA reveals a tetramer of toxin-antitoxin heterodimers containing pin domains and ribbon-helix-helix motifs. *J. Biol. Chem.*, **281**, 37942–37951.
31. Ogura,T., Whiteheart,S.W. and Wilkinson,A.J. (2004) Conserved arginine residues implicated in ATP hydrolysis, nucleotide-sensing, and inter-subunit interactions in AAA and AAA+ ATPases. *J. Struct. Biol.*, **146**, 106–112.
32. Kettenberger,H., Armache,K.J. and Cramer,P. (2004) Complete RNA polymerase II elongation complex structure and its interactions with NTP and TFIIS. *Mol. Cell*, **16**, 955–965.
33. Sigurdsson,S., Dirac-Svejstrup,A.B. and Svejstrup,J.Q. (2010) Evidence that transcript cleavage is essential for RNA polymerase II transcription and cell viability. *Mol. Cell*, **38**, 202–210.
34. Vassylyev,D.G., Svetlov,V., Vassylyeva,M.N., Perederina,A., Igarashi,N., Matsugaki,N., Wakatsuki,S. and Artsimovitch,I. (2005) Structural basis for transcription inhibition by tagetitoxin. *Nat. Struct. Mol. Biol.*, **12**, 1086–1093.